[Article] www.whxb.pku.edu.cn

混合稀电解质条件下合成球状 SBA-15 粒子

王月娟 金炜阳 王雪俐 金凌云 鲁继青 罗孟飞*
(浙江师范大学物理化学研究所, 浙江省固体表面反应化学重点实验室, 浙江 金华 321004)

摘要: 在酸性合成法基础上, 不添加有机共溶剂和其它模板剂, 通过加入少量 NH_4F 和 $Cu(NO_3)_2$ 得到了分散的球状形貌 SBA-15 粒子. 对所得样品用小角 X 射线衍射(XRD)、N_2 吸脱附曲线、扫描电镜(SEM)进行表征, 讨论了不同电解质对样品形貌和孔结构的影响. 结果发现, 随着酸浓度增加, 得到了分散的规则六边形 SBA-15 粒子, 而加入一定量的氟化铵则得到了球形纠结状形貌的 SBA-15. 实验表明, 氟离子在形成球状粒子的过程中起主要作用, 而 Cu^{2+}阻碍了球状粒子的纠结. 随着 Cu^{2+}浓度的增加, 部分硅源不能参与自组装生成 SBA-15, 其原因可能是 Cu^{2+}与模板剂中亲水的聚氧乙烯形成 PEO/Cu^{2+}端基, 影响了硅源正常的缩聚.

关键词: SBA-15; 球状; 电解质; 形貌
中图分类号: O647

Synthesis of Spherical SBA-15 Particles under Mixed and Dilute Electrolyte Conditions

WANG Yue-Juan JIN Wei-Yang WANG Xue-Li JIN Ling-Yun LU Ji-Qing LUO Meng-Fei*
(*Zhejiang Key Laboratory for Reactive Chemistry on Solid Surfaces, Institute of Physical Chemistry, Zhejiang Normal University, Jinhua 321004, Zhejiang Province, P. R. China*)

Abstract: Spherical SBA-15 particles were synthesized by co-addition of dilute but strong electrolytes (NH_4F and $Cu(NO_3)_2$) under classical acidic conditions without an organic solvent or another template. These materials were characterized by low angle X-ray diffraction (XRD), N_2 sorption isotherms, and scanning electron microscopy (SEM). Separated uniform hexagonal SBA-15 particles form in strong acidic media while an appropriate content of fluoride anions favors the synthesis of a sphere-like and highly pored ordered structure. Effects of different electrolytes on the morphology and the mesostructure of the resulting materials were discussed. We found that fluoride played the main role in the formation of sphere-like SBA-15 while the presence of the Cu^{2+} was beneficial for the formation of separated spherical SBA-15 particles. When the concentration of Cu^{2+} increases, a part of the silica does not contribute to the formation of SBA-15. This phenomenon is probably due to the formation of a PEO (polyoxyethylene)/Cu^{2+} head-group at the hybrid interface which affects the normal coordination and condensation of the silica source.

Key Words: SBA-15; Spherical; Electrolyte; Morphology

The discovery of SBA-15 mesoporous silica materials has attracted a lot of interest due to its high surface area, uniform pore distribution, large pore size, and highly valuable potential applications in the fields of catalysis, separation, and adsorption[1–3]. A precise control over the morphology is required to realize the promising applications of this material[4–6]. For example, fiberlike SBA-15 has superior dynamic volatile organic compounds (VOCs) adsorption capacities than that of rodlike SBA-15[7], while spherical particles can be used in high-performance liquid chromatography as the stationary phase[8]. Therefore, synthesis of mesoporous materials with controllable morphologies is desirable.

Received: February 23, 2009; Revised: April 29, 2009; Published on Web: May 18, 2009.
*Corresponding author. Email: mengfeiluo@zjnu.cn; Tel: +86-579-82283910.
The project was supported by the Natural Science Foundation of Zhejiang Province, China (202131).
浙江省自然科学基金(202131)资助项目

Recently, there are many reports describing methods for controlling the shapes of mesoporous materials by using various surfactants as the structure-directing agent. Effects of synthetic conditions on the macrostructures of the materials, such as silica source, acidity, reactant molar ration, cosolution, cosurfactant, and inorganic salts, were investigated. Mesoporous silica in forms of fibers[9], gyroids and discoids[4], films[10] and spheres[8,9] have been synthesized using ionic surfactants or block copolymers. Factors like free energy[11], polarity[9], and ionic effects[12,13] were considered to explain the formation mechanism of different shapes and curved morphologies of mesoporous silica.

In general, mesoporous ordered silica spheres were synthesized in presence of ionic surfactants or nonionic cosurfactants[9,14–16]. Mesoporous SBA-15 with uniform spherical particle is comparatively difficult to be obtained through changing stirring condition, operation temperature, or material composition ratio. Therefore, electrolytes are always introduced in the synthesis process[9,11,17]. In order to affect the macrostructure of materials, a relatively high electrolytes/silica sources molar ratio was used[9,11,17]. Until now, spherical silica particles synthesized under mixed dilute electrolytes conditions has not been reported.

In this work, we synthesized spherical SBA-15 using nonionic surfactant triblock polymer Pluronic 123 (P123) as an unique template. Ammonium fluoride (NH_4F) and cupric nitrate ($Cu(NO_3)_2$) were used to control the morphologies of mesoporous silica particles. The effect of the acidity on the morphology during the preparation was also studied.

1 Experimental

1.1 Syntheses of materials

SBA-15 particles were synthesized following the procedure published in the literature[18]: triblock polymer $EO_{20}PO_{70}EO_{20}$ (P123, Aldrich) was used as the template, tetraethyl orthosilicate (TEOS, 98%, Aldrich) as the silicon source, and a certain amount of strong electrolyte (NH_4F, $Cu(NO_3)_2$) was added into the homogeneous surfactant-water solution. The molar composition of the TEOS:P123:NH_4F:$Cu(NO_3)_2$:HCl:H_2O mixture was 1:0.017:0.05:(0.01–0.05):5.88:203. After the pH adjustment, the resulting solution was stirred at 37 ℃ for 20 h, and then it was transferred to a teflon-lined autoclave to age at 100 ℃ for 24 h under static conditions. The solid product was filtered and washed with deionized water and ethanol. The obtained solid was dried at 90 ℃ for another 24 h, followed by calcination at 550 ℃ for 8 h. The samples were denoted as S-x, where the x represents the synthetic conditions of the materials. The synthetic parameters and nomination of the samples are listed in Table 1.

1.2 Characterizations

X-ray diffraction (XRD) patterns were collected on a PANAlytical PRO MPD automated powder diffractometer equipped with a X′celerator detector using Cu K_α radiation (λ=0.1541 nm), with a working voltage of 40 kV and a working current of 40 mA. N_2 sorption isotherms were obtained using a Quantachrome Autosorb-1 apparatus at liquid nitrogen temperature (77 K). Scanning electron microscopy (SEM) images were obtained on a Hitachi S-4800 field emission microscope. Transmission electron microscopy (TEM) image was obtained on a JEM2010 microscope operated at 200 kV.

Table 1 Sample nomination and their synthesis conditions

Sample	pH	n_F/n_{TEOS}	n_{Cu}/n_{TEOS}
S-0	0*	–	–
S-1	1	–	–
S-1F	1	0.05	–
S-1Cu0.01	1	–	0.01
S-1FCu0.01	1	0.05	0.01
S-1FCu0.03	1	0.05	0.03
S-1FCu0.05	1	0.05	0.05

*pH=0 means that $[H^+]$ is 1 mol·L^{-1} in the initial homogeneous solution.

The copper contents of these samples were analyzed by atomic absorption spectroscopy (AAS) using a Perkin Elmer Analyst 800 double beam spectrometer. The AAS results showed that no copper atoms were incorporated into the samples.

2 Results and discussion

Fig.1 shows the low angle XRD patterns of the materials prepared under different conditions. For the samples prepared without the addition of NH_4F and $Cu(NO_3)_2$, the XRD patterns exhibit three well-resolved peaks, which are assigned to the (100), (110), and (200) reflections of a hexagonal planar symmetry (*P6mm*). The XRD pattern of S-1F confirms that proper content of fluoride introduced into the solution favors to obtain well-defined mesostructures[19]. Compared with S-0, S-1 and S-1F, for S-1Cu0.01, the intensity of the (100) peak decreases with the introduction of proper Cu^{2+} ions, implying a partial damage to the *P6mm* hexagonal structure. However, it seems that there is no finely hexagonal structure when Cu^{2+} and F^- ions co-exist in solutions, since for these materials only the (100) reflection maintains with a decreased intensity (curves e–g).

Fig.2 shows nitrogen adsorption-desorption isotherms of the materials. Specific surface area was calculated using BET method. Pore size distribution was calculated using the BJH formula applied to the adsorption part of the isotherm. The

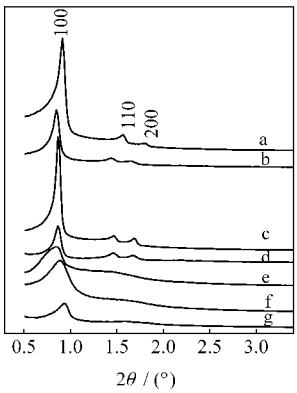

Fig.1 Low-angle XRD patterns of samples
(a) S-0, (b) S-1, (c) S-1F, (d) S-1Cu0.01, (e) S-1FCu0.01, (f) S-1FCu0.03, (g) S-1FCu0.05

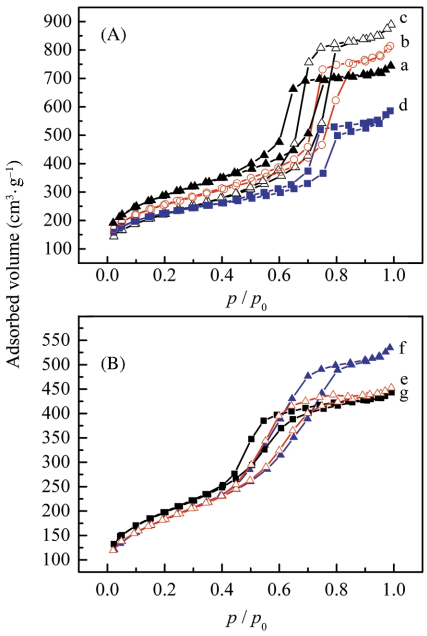

Fig.2 Nitrogen adsorption-desorption isotherms of samples
(a) S-0, (b) S-1, (c) S-1F, (d) S-1Cu0.01, (e) S-1FCu0.01, (f) S-1FCu0.03, (g) S-1FCu0.05

isotherms of all samples are of type IV with a sharp adsorption branch located at relative pressures in the range of 0.45 to 0.80, which is the characteristic of mesoporous materials corresponding to the capillary condensation of N_2 in primary mesopores. The textural properties of the samples are listed in Table 2.

Compared with the samples synthesized in NH_4F or $Cu(NO_3)_2$, the isotherms of the S-1FCu samples (Fig.2(B) curves, e–g) do not exhibit a sharp step as N_2 condensation step shown in Fig.2

Table 2 Textural parameters of the materials prepared under different conditions

Sample	S_{BET}/($m^2 \cdot g^{-1}$)	V_T/($cm^3 \cdot g^{-1}$)	d_{100}/nm	D_p/nm	t_{wall}/nm
S-0	1030	1.13	9.7	7.9	3.2
S-1	912	1.25	10.4	9.4	2.6
S-1F	788	1.39	10.2	9.4	2.4
S-1Cu0.01	814	0.86	10.4	9.6	2.6
S-1FCu0.01	697	0.68	10.4	4.3	7.7
S-1FCu0.03	646	0.71	9.8	5.5	5.9
S-1FCu0.05	648	0.84	9.5	7.7	4.3

V_T: total pore volume; d_{100}: (100) interplanar spacing; D_p: mesopore size calculated using the BJH procedure; t_{wall}: silica wall thickness calculated by a_0-D_p, $a_0=2\times d_{100}/\sqrt{3}$

(A), indicating that the mesoporous structure in these particles may not be so uniform as expected. In contrast to the S-1, the S-1Cu0.01 synthesized under dilute Cu^{2+} solution, there is not only a much lower intensity of (100) reflection but also lower mesoporous volume, which implies that Cu^{2+} ions have an opposite effect on the formation of the ordered pore structure. The largest N_2 condensation in primary mesopores of the sample S-1F further indicates that fluoride could lead to an ordered pore structure and larger mesopore volume. The data in Table 2 suggest that the different molar ratios of Cu/F have strong effects on the fraction of pore size and wall thickness, with a higher Cu/F molar ratio resulting in a larger main pore size and a thinner thickness of the corresponding wall.

Fig.3 shows the SEM images of the materials. The material S-0 prepared under strong acidity (Fig.3a) contains hexagonal prism with side-length of about 0.5 μm and height of about 0.6 μm. When the pH value of the solution raises up to 1.0, as shown in Fig.3b, the resulting hexagonal prisms are stretched and dis-

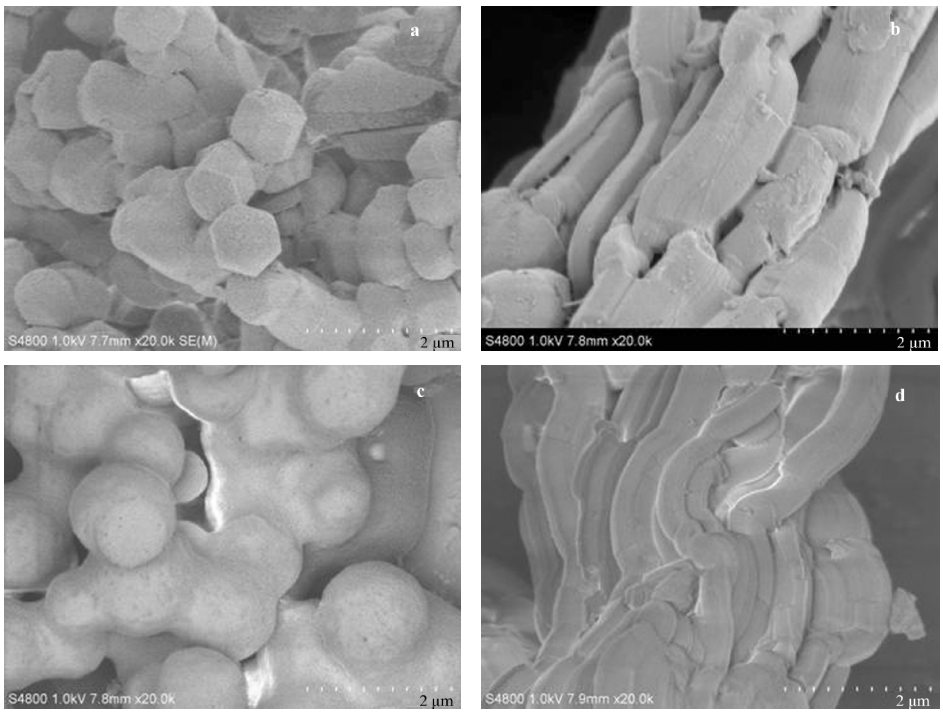

Fig.3 SEM images of samples (a) S-0, (b) S-1, (c) S-1F, and (d) S-1Cu0.01

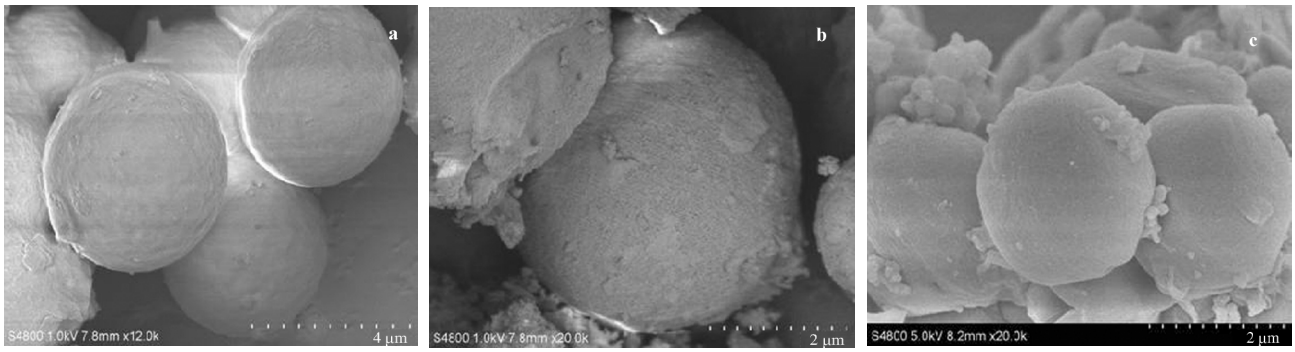

Fig.4 SEM images of materials prepared under mixed electrolyte conditions

(a) S-1FCu0.01, (b) S-1FCu0.03, (c) S-1FCu0.05

torted, and intertwined with each other. This tendency is in well accordance with those results described in detail elsewhere[4]. A similar shape transform has also been observed in cation surfactant template systems reported by Naik *et al.*[20]. The explanation is that for the solution with pH=0, the silica condensation rate is much slower than that with pH=1. While tetramethylorthosilicate (TMOS) is used as the silica source, only fiber-like macroscopic structure is obtained as a result of a faster silica condensation rate[9].

Electrolytes can also modify the morphology of corresponding material. For the S-1F, junction-spheres (Fig.3c) are obtained when NH_4F is added into the acidic solution (pH=1.0), which is different from the morphology of the S-1. However, when $Cu(NO_3)_2$ is added into this acidic solution, the surface of the S-1Cu0.01, is smoother (Fig.3d) than that of the S-1.

Fig.4 shows the SEM images of the materials prepared under mixed electrolyte solution. Spherical particles are obtained when both NH_4F and $Cu(NO_3)_2$ are added. It can be seen from Fig.4 that with increasing concentration of $Cu(NO_3)_2$, some silica oddments possessing irregular shape are observed (b and c). On the basis of the previous reports[12,19] and our present experimental results, it is believed that the fluoride plays a key role in the formation of the sphere-like morphology in the materials, while Cu^{2+} ions are regarded as a "regulator" in the synthesis process.

Fig.5 shows the TEM image of the S-1FCu0.01 sample. One dimensional pores can be clearly observed. Meanwhile, the pore size is 4.4 nm, which is consistent with the N_2 adsorption result.

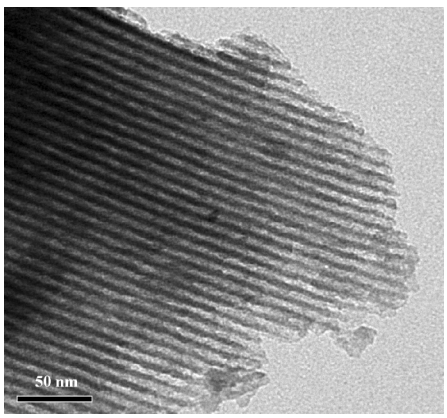

Fig.5 TEM image of S-1FCu0.01 sample

The interface of nonionic PEO-based surfactant micelles is not like the quaternary ammonium surfactants, but more like a water-rich corona interphase[21]. The water located at the interface is more nucleophilic than bulk water due to the strong H-bonding interactions between the water and the EO groups. The introduction of Cu^{2+} ions will accelerate the formation of PEO/Cu^{2+} head-group, which leads to the previously nucleophilic PEO units and is not favorable for the coordination and condensation of silica source, even with the presence of F^- anions[12]. The addition of Cu^{2+} ions makes junction-spheres separate from each other. With increasing Cu^{2+} ion concentration, the large amount of PEO/Cu^{2+} head-group seriously hinder the effective assembly between the silicon source and template, which results in forming some silica oddments in synthesis process. Furthermore, the higher Cu/F ratio in the synthesis solution, the material with thinner wall thickness is obtained. In addition, the formation of PEO/Cu^{2+} head-group probably leads to the poor ordered pore structure of the silica materials.

3 Conclusions

The effects of dilute electrolytes (NH_4F, $Cu(NO_3)_2$) on the morphologies and pore structure of mesoporous silica materials were investigated. The rate of silica hydrolysis and condensation plays the dominant role in the preparation of spherical mesoporous silica. The addition of dilute fluoride is favorable for the formation of the spherical morphology while Cu^{2+} hinders the silica condensation.

References

1 Kruk, M.; Jaroniec, M. C.; Ko, C. H.; Ryoo, R. *Chem. Mater.*, **2000, 12**: 1961

2 Newalkar, B. L.; Choudary, N. V.; Turaga, U. T.; Vijayalakshmi, R. P.; Kumar, P.; Komarneni, S.; Bhat, T. S. G. *Chem. Mater.*, **2003, 15**: 1474

3 Zhao, H. L.; Hu, J.; Wang, J. J.; Zhou, L. H.; Liu, H. L. *Acta Phys. -Chim. Sin.*, **2007, 23**: 801 [赵会玲, 胡 军, 汪建军, 周丽绘, 刘洪来. 物理化学学报, **2007, 23**: 801]

4 Yang, H.; Coombs, N.; Ozin, G. A. *Nature*, **1997, 386**: 692

5 Zhao, D.; Yang, P.; Melosh, N.; Feng, J.; Chmelka, B. F.; Stucky, G. D. *Adv. Mater*., **1998, 10**: 1380

6 Sokolov, I.; Yang, H.; Ozin, G. A.; Kresge, C. T. *Adv. Mater*., **1999, 11**: 636

7 Kosuge, K.; Kubo, S.; Kikukawa, N.; Takemori, M. *Langmuir*, **2007, 23**: 3095

8 Ma, Y.; Qi, L.; Ma, J.; Wu, Y.; Liu, O.; Cheng, H. *Colloids Surf. A*, **2003, 229**: 1

9 Zhao, D.; Sun, J.; Li, Q.; Stucky, G. D. *Chem. Mater*., **2000, 12**: 275

10 Miyata, H.; Noma, T.; Watanabe, M.; Kuroda, K. *Chem. Mater*., **2002, 14**: 766

11 Yu, C.; Fan, J.; Tian, B.; Zhao, D. *Chem. Mater*., **2004, 16**: 889

12 Bagshaw, S. A. *J. Mater. Chem*., **2001, 11**: 831

13 Leontidis, E. *Curr. Opin. Colloid Interface Sci*., **2002, 7**: 81

14 Yang, L.; Wang, Y.; Luo, G.; Dai, Y. *Particuology*, **2008, 6**: 143

15 Mesa, M.; Sierra, L.; López, B.; Ramirez, A.; Guth, J. L. *Solid-State Sci*., **2003, 5**: 1303

16 Stevens, W. J. J.; Lebeau, K.; Mertens, M.; Tendeloo, G. V.; Cool, P.; Vansant, E. F. *J. Phys. Chem. B*, **2006, 110**: 9183

17 Jin, Z.; Wang, X.; Cui, X. *Colloids Surf. A*, **2008, 316**: 27

18 Zhao, D.; Feng, J.; Huo, Q.; Melosh, N.; Fredrickson, G. H.; Chmelka, B. F.; Stucky, G. D. *Science*, **1998, 279**: 548

19 Li, Y.; Zhang, W.; Zhang, L.; Yang, Q.; Wei, Z.; Feng, Z.; Li, C. *J. Phys. Chem. B*, **2004, 108**: 9739

20 Naik, S. P.; Elangovan, S. P.; Okubo, T.; Sokolov, I. *J. Phys. Chem. C*, **2007, 111**: 11168

21 Edler, K. J.; Reynolds, P. A.; White, J. W.; Cookson, D. *J. Chem. Soc. Faraday Trans*., **1997, 199**: 93